Structure of the magnetized sheath of a dusty plasma

H. Mehdipour, I. Denysenko, and K. Ostrikov

Citation: Physics of Plasmas (1994-present) **17**, 123708 (2010); doi: 10.1063/1.3526740
View online: http://dx.doi.org/10.1063/1.3526740
View Table of Contents: http://scitation.aip.org/content/aip/journal/pop/17/12?ver=pdfcov
Published by the AIP Publishing

Structure of the magnetized sheath of a dusty plasma

H. Mehdipour,[1] I. Denysenko,[2] and K. Ostrikov[3]
[1]*Department of Physics, Faculty of Science, Sahand University of Technology, Tabriz 51335-1996, Iran*
[2]*School of Physics and Technology, V. N. Karazin Kharkiv National University, 4 Svobody sq., Kharkiv 61077, Ukraine*
[3]*Plasma Nanoscience Centre Australia (PNCA), CSIRO Materials Science and Engineering, P.O. Box 218, Lindfield, New South Wales, Sydney 2070, Australia and School of Physics, The University of Sydney, Sydney, New South Wales 2006, Australia*

(Received 8 November 2010; accepted 23 November 2010; published online 9 December 2010)

A three-component fluid model for a dusty plasma-sheath in an oblique magnetic field is presented. The study is carried out for the conditions when the thermophoretic force associated with the electron temperature gradient is one of the most important forces affecting dust grains in the sheath. It is shown that the sheath properties (the sheath size, the electron, ion and dust particle densities and velocities, the electric field potential, and the forces affecting the dust particles) are functions of the neutral gas pressure and ion temperature, the dust size, the dust material density, and the electron temperature gradient. Effects of plasma-dust collisions on the sheath structure are studied. It is shown that an increase in the forces pushing dust particles to the wall is accompanied by a decrease in the sheath width. The results of this work are particularly relevant to low-temperature plasma-enabled technologies, where effective control of nano- and microsized particles near solid or liquid surfaces is required. © *2010 American Institute of Physics*. [doi:10.1063/1.3526740]

I. INTRODUCTION

As a unique multicomponent system, dusty (complex) plasmas have attracted a major interest in the last few decades. It has been actively studied in laboratory, industrial and astrophysical situations.[1–5] At present, properties of such plasmas, including collective phenomena, dust generation and charging, formation of complex self-organized structures (dust crystals, voids, vortices, dust balls, etc.), and forces affecting dust particles are reasonably well understood.[1–11]

It has also been studied how dust particles affect other plasma particles (their densities, spatial distributions, drift velocities, electron energy distribution function, and temperature). In particular, it was shown that the presence of dust particles in laboratory plasmas is usually accompanied by a decrease of the electron density and an increase of the electron temperature.[1,12] Dust particles also affect the shape of the electron energy distribution function,[13–15] as well as the plasma-sheath.[16]

The presence of dense clouds of dust particles near the wall essentially changes the plasma-sheath behavior and a new dissipative sheath structure can be formed.[2] The dust particles can be introduced artificially in a plasma-sheath or may appear as the impurity contaminants, which are added by production tools and processes. In plasma-assisted fabrication of microchips, the dust contaminant is a serious threat, and the dust particles must be removed from the plasma environment; otherwise the unwanted contaminant compromises the performance and quality of the microchip. In technologies, where plasma-grown nanoparticles are building units for nanostructures formed on a substrate, the dust particles cross the sheath before their deposition on the substrate. A precise manipulation of these building units in the sheath is required,[17–23] which is impossible without understanding processes in the dusty sheath.

The dynamics of the dust component in the plasma-sheath, both an isolated grain and a dense cloud of dust particles, has been studied by several authors.[24–31] Most of the studies have been carried out for the case when an external magnetic field is absent. Ma and Yu[27] showed that there exists a critical velocity for ions (similar to the Bohm criterion for two-component plasma) entering the sheath, which is a function of dust density. They also found that the potential drop near the wall is small (the sheath is wider) for intermediate values of dust density than that of the dust-free case, while at large density the potential drop is larger (the sheath is narrower). A self-consistent relation between the dust surface potential and ion Mach number at the sheath edge was derived in Ref. 30. Chutov and co-workers[32] showed that dust particles due to selective collection of electrons and ions can cause essential change in both electron and ion distribution functions, as well as ion flux into the sheath. A dusty plasma-sheath was also simulated in the presence of two temperature electrons.[33] It was shown numerically that trapped dust grains play an important role in sheath modification leading to the formation of triple electric field structure within the sheath and construction of the sheath.[34] The Bohm criterion for the electrostatic sheath in electronegative dusty plasmas, which are composed of electrons, negative and positive ions, as well as dust grains, was investigated in Ref. 35. Mikikian *et al.*[36] measured the dust charge in the sheath in a dc discharge plasma. The influence of different dust density as well as of the negative bias to the metallic plate on the ion sheath structure was studied experimentally in Ref. 37.

Magnetized plasma-sheaths with dust particles have been also intensively studied. It was shown that the equilibrium and levitation of dust particles in a collisional magnetized sheath depends on plasma-neutral collision frequencies

and on the magnetization, if the ambient magnetic field is parallel to the wall.[38] The structure of a plasma-sheath and dynamics of a dust particle embedded in the sheath in the presence of an oblique magnetic field were investigated in Refs. 39 and 40. Considering the Boltzmann response of the ions and electrons in plasma dynamics and inertial dynamics of the dust charged grains embedded in a constant magnetic field, the nature of the electrostatic potential near a plasma boundary was previously reported.[41] The effects of the magnitude of the oblique magnetic field, the dust and plasma number densities, and the electron temperature on the sheath structure and spatial distributions of various sheath parameters were also studied.[42] A magnetized sheath of a dusty plasma was investigated via numerical solution of stationary multifluid equations by taking into account the electric, magnetic, gravitational, ion drag, neutral drag forces, and the thermophoretic force associated with neutral gas temperature gradient.[43] Meanwhile, properties of a magnetized sheath under the conditions, when the thermophoretic force associated with the electron temperature gradient is one of the most important forces affecting dust grains, have not been studied.

In this paper, we study a dusty plasma-sheath in the presence of an oblique magnetic field. To investigate the behavior of the structure, a three-component fluid model is developed. The case, when the dust charge density is larger than the electron density, is considered. Studying the dust particle behavior in the sheath, we account for most important forces affecting dust grains: the electric and ion drag forces, thermophoretic force associated with neutral gas temperature gradient and the gravitational force. We also account for effects of the thermophoretic force associated with electron temperature gradient,[44] which can be important in low-pressure high-density plasmas, when the ratio of the electron density to the neutral gas density and the electron temperature gradients are large. An example of the plasma, where the force can be important, is electron cyclotron plasma. We investigate how the magnetized sheath parameters (the sheath size, the electron, ion, and dust particle spatial distributions, the dust particle and ion velocities, the dust charge, the electric potential, and the forces affecting dust particles) depend on dust particle radius, dust material density, neutral gas pressure, ion temperature, and electron temperature gradient.

This article is organized in the following fashion. In Sec. II, the multifluid model and main assumptions of the model are introduced. The numerical results on the study of the sheath structure are presented in Sec. III. The article concludes in Sec. IV with the discussion and summary of the results.

II. THEORETICAL MODEL AND BASIC EQUATIONS

In this section, we present a theoretical model for a plasma-sheath with dust particles in an oblique magnetic field. We consider the case of an argon discharge sustained near a planar electrode (Fig. 1). The gas discharge consists of positive single-charged ions with density n_i, electrons with density n_e, and dust particles with density n_d, dust radius r_d and charge Z_d, as well as of neutral argon atoms with density n_n. The gas discharge may be separated into two regions, the plasma bulk, where the plasma is quasineutral, and the sheath layer, where the total charge density is not equal to zero.

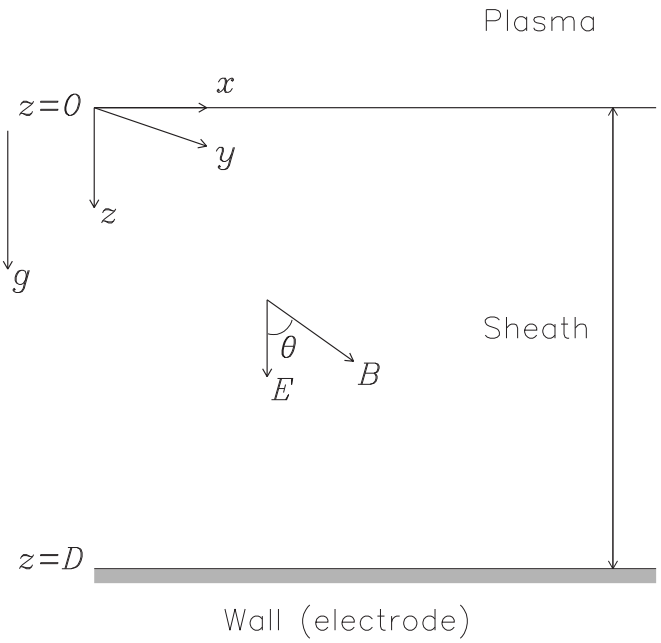

FIG. 1. The geometry of the magnetized plasma-sheath.

The plasma-sheath boundary is located at $z=0$, where the electrostatic potential is assumed to be zero. The electrode (wall) is sustained at the potential ϕ_w and is located at $z=D$. The steady-state magnetic field $\vec{B}$ makes an angle θ with the z-axis. We consider the case when the neutral gas and electron temperatures are nonuniform in the z-direction and the ion temperature is assumed to be equal to the gas temperature. The dust particles in the discharge are affected by different forces such as the electric, Lorentz, gravitational, ion and neutral drag forces, and the thermophoretic force. It is assumed that the gravitational force is directed in the z-direction (to the wall).

To describe the densities and velocities of electrons, ions, and dust particles, we use a multicomponent fluid approach.[45–47] In this approach, the densities of the charged particles are described by the continuity equations

$$\frac{d}{dz}(n_d v_{dz}) = 0, \tag{1}$$

$$\frac{d}{dz}(n_i v_{iz}) = \gamma_{\text{ion}} n_n n_e - \nu_{id}^c n_d, \tag{2}$$

$$\frac{d}{dz}(n_e v_{ez}) = \gamma_{\text{ion}} n_n n_e - \nu_{ed}^c n_d, \tag{3}$$

where v_{jz} is the z-component of species j ($j=d,i,e$ for dust particles, ions, and electrons, respectively). γ_{ion} is the rate for ionization of ground-state atoms. We take the rate in the form[48] $\gamma_{\text{ion}}=5\times10^{-8}\exp(-15.8/T_e)$ s^{-1} (here T_e is the electron temperature in eV). ν_{jd}^c is the frequency with which the species j attach to a dust grain. The expressions for ν_{jd}^c will be given below.

The velocities of charged particles in the sheath are described by the momentum equations, for the dust particles,

$$m_d v_{dz}\frac{dv_{dx}}{dz} = \frac{eZ_d}{c}Bv_{dy}\cos\theta + F_{idx} + F_{ndx}, \tag{4}$$

$$m_d v_{dz}\frac{dv_{dy}}{dz} = \frac{eZ_d}{c}B(v_{dz}\sin\theta - v_{dx}\cos\theta) + F_{idy} + F_{ndy}, \tag{5}$$

$$m_d v_{dz}\frac{dv_{dz}}{dz} = -eZ_d\left(\frac{d\phi}{dz} + \frac{B}{c}v_{dy}\sin\theta\right) + F_{idz} + F_{ndz} + F_{thz} + m_d g, \tag{6}$$

for the ions

$$m_i v_{iz}\frac{dv_{ix}}{dz} = \frac{e}{c}Bv_{iy}\cos\theta - m_i\nu_{in}v_{ix} - m_i\nu_{id}^e v_{ix}, \tag{7}$$

$$m_i v_{iz}\frac{dv_{iy}}{dz} = \frac{e}{c}B(v_{iz}\sin\theta - v_{ix}\cos\theta) - m_i\nu_{in}v_{iy} - m_i\nu_{id}^e v_{iy}, \tag{8}$$

$$m_i v_{iz}\frac{dv_{iz}}{dz} = -e\left(\frac{d\phi}{dz} + \frac{B}{c}v_{iy}\sin\theta\right) - \frac{T_i}{n_i}\frac{dn_i}{dz} - m_i\nu_{in}v_{iz} - m_i\nu_{id}^e v_{iz}, \tag{9}$$

and for the electrons

$$0 = -\frac{e}{c}Bv_{ey}\cos\theta - m_e\nu_{en}v_{ex} - m_e\nu_{ed}^e v_{ex}, \tag{10}$$

$$0 = -\frac{e}{c}B(v_{ez}\sin\theta - v_{ex}\cos\theta) - m_e\nu_{en}v_{ey} - m_e\nu_{ed}^e v_{ey}, \tag{11}$$

$$0 = e\left(\frac{d\phi}{dz} + \frac{B}{c}v_{ey}\sin\theta\right) - \frac{1}{n_e}\frac{d}{dz}(n_e T_e) - m_e\nu_{en}v_{ez} - m_e\nu_{ed}^e v_{ez}, \tag{12}$$

where e is the elementary charge, ϕ is the electrostatic potential, g is the gravitational constant, and c is the speed of light. m_j is the mass, v_{jx}, v_{jy}, and v_{jz} are the x-, y-, and z-components of the velocity of the species j. $\nu_{in}(\nu_{en})$ and $\nu_{id}^e(\nu_{ed}^e)$ are the momentum-transfer rates for ion (electron)-neutral and ion (electron)-dust collisions, respectively. $F_{id\alpha}$, $F_{nd\alpha}$, and $F_{th\alpha}$ are the $\alpha(=x,y,z)$ components of the ion and neutral drag forces and the thermophoretic force, respectively. T_e and T_i are the electron and ion temperatures, respectively.

The momentum-transfer rates ν_{jn} and ν_{jd}^e in Eqs. (7)–(12) were determined using the expressions[13] $\nu_{jn}=n_n\sigma_{jn}V_{tj}$ and $\nu_{jd}^e=n_d\sigma_{jd}^e V_{tj}$, where σ_{jn} and σ_{jd}^e are the cross sections for collisions of electrons or ions with neutral and dust particles, respectively. In our calculations, $\sigma_{in}=5.0\times10^{-15}$ cm^2, $\sigma_{en}=5.4\times10^{-16}$ cm^2,[49] and $\sigma_{jd}^e=\pi r_d^2(2e^2Z_d/m_j r_d V_{tj}^2)^2 e^{2r_d/\lambda_D}\ln\Lambda_j$, where $\Lambda_j\approx|-\lambda_D m_j V_{tj}^2/r_d e\phi_d|$, $V_{tj}=[\bar{v}_j^2+8T_j/(\pi m_j)]^{1/2}$ is the total velocity of the jth particle and ϕ_d is the dust surface potential. $\lambda_D=\lambda_{De}\lambda_{Di}/(\lambda_{De}^2+\lambda_{Di}^2)^{1/2}$ is the plasma Debye radius, where $\lambda_{De}=\sqrt{T_e/4\pi n_e e^2}$ and $\lambda_{Di}=\sqrt{T_i/4\pi n_i e^2}$ are the electron and ion Debye radii, respectively.

The electrostatic potential ϕ is governed by the Poisson equation,

$$\frac{d^2\phi}{dz^2} = 4\pi e(n_e - n_i - Z_d n_d). \tag{13}$$

At the plasma-sheath boundary, the densities of charged particles are connected by the quasineutrality condition

$$n_{i0} - n_{e0} + Z_{d0}n_{d0} = 0, \tag{14}$$

where n_{i0}, n_{e0}, n_{d0}, and Z_{d0} are the ion, electron, and dust particle densities and dust charge at $z=0$, correspondingly.

The ion drag force, affecting a dust grain, may be divided on two components, the collection force

$$\boldsymbol{F}_{id}^{\rm coll} = \pi r_d^2 n_i m_i V_{ti}\bar{\boldsymbol{v}}_i\left(1 - \frac{2e^2Z_d}{r_d m_i V_{ti}^2}\right) \tag{15}$$

and the orbit force

$$\boldsymbol{F}_{id}^{\rm orb} = 2\pi b_0^2 n_i m_i V_{ti}\bar{\boldsymbol{v}}_i\ln\left(\frac{b_0^2+\lambda_D^2}{b_0^2+b_c^2}\right), \tag{16}$$

where $\bar{\boldsymbol{v}}_i=\boldsymbol{v}_i-\boldsymbol{v}_d$ is the ion velocity with respect to the dust particle, $b_0=e^2Z_d/(m_i v_i^2)$ and $b_c=r_d(1-2b_0/r_d)^{1/2}$.

For the typical ratio $v_d/v_{\rm th}\ll1$ (where $v_{\rm th}=\sqrt{T_n/m_n}$, while T_n and m_n are the neutral gas temperature and mass, respectively), the neutral drag force $\boldsymbol{F}_{nd}$ is given by[39]

$$\boldsymbol{F}_{nd} = -\tfrac{8}{3}\sqrt{2\pi}r_d^2 m_n n_n v_{tn}\boldsymbol{v}_d. \tag{17}$$

The total thermophoretic force $\boldsymbol{F}_{\rm th}=\boldsymbol{F}_{{\rm th},n}+\boldsymbol{F}_{{\rm th},e}$ can be split into two components originating from the electron and neutral temperature gradients. The thermophoretic force associated with the neutral temperature gradient $\nabla_z T_n$ is

$$\boldsymbol{F}_{{\rm th},n} \approx -\frac{5}{4\sqrt{2}}\left(\frac{r_d}{\sigma_{\rm LJ}}\right)^2\nabla_z T_n, \tag{18}$$

where $\sigma_{\rm LJ}$ ($\approx3.4\times10^{-8}$ cm) is the Lennard-Jones collision diameter of the gas.

The thermophoretic force associated with electron temperature gradient may be approximated by[44]

$$\boldsymbol{F}_{{\rm th},e} \approx -\frac{8\sqrt{2}}{15}\frac{\lambda_D^2 n_e}{\sigma_{en}n_n}\nabla_z T_e. \tag{19}$$

Expression (19) is obtained assuming that the screened length of the electric field around dust particles is about the Debye length, which is applicable only for relatively small dust particles ($r_d<1$ μm).[1]

To calculate the electric and ion drag forces and the rates describing electron (ion)-dust interactions, we need to know the dust charge Z_d as a function of coordinate z. The dust charge can be obtained by balancing the electron and ion grain currents,

$$I_e + I_i = 0, \tag{20}$$

where the electron grain current, I_e, is given by

$$I_e = -\pi r_d^2 n_e e V_{te} f(Z_d), \tag{21}$$

where $f(Z_d)=\exp(e^2 Z_d / r_d T_e)$ for $Z_d<0$ and $f(Z_d)=1+e^2 Z_d / r_d T_e$ for $Z_d>0$.

The ion current to a negatively charged dust grain is approximated by[50]

$$I_i = \pi r_d^2 n_i e V_{ti}(1 - \xi + H\xi^2 \lambda_D/\lambda_{\mathrm{mfp}}), \tag{22}$$

where $\lambda_{\mathrm{mfp}}=1/(n_n\sigma_{in})$ is the ion mean free path and $\xi=2e^2 Z_d/(r_d m_i V_{ti}^2)$. The function H has the following asymptotes: $H\approx 0.1$ for $0.1\le\beta\le 10$, $H\approx\beta$ for $\beta\ll 1$, and $H\approx\beta^{-2}(\ln\beta)^3$ for $\beta\gg 1$, where $\beta=2|e^2 Z_d|/(\lambda_D m_i V_{ti}^2)$.[50]

For positively charged dust grains, the ion current is determined by

$$I_i = \pi r_d^2 n_i e V_{ti} \exp[-2e^2 Z_d/(r_d m_i V_{ti}^2)]. \tag{23}$$

The dust charging theory can be used if the distance between grains d (which is about n_d^{-3}) is larger than the ion Debye length. On the other hand, the fluid model for dust dynamics requires that the intergrain distance be smaller than the electron Debye length. For typical plasma parameters considered here ($n_{i0}\approx n_{e0}=10^{10}$ cm^{-3}, $T_e=3$ eV, and $T_i=0.05$ eV), the theoretical model is applicable in the dust density range 4.6×10^5 cm$^{-3}<n_d<8.8\times 10^8$ cm^{-3}.

Note also that the dust charging theory may be used only if the dust radius r_d is smaller than the electron gyroradius, i.e., the magnetic field B must be smaller than a critical value B_{cr} determined by[51]

$$B_{\mathrm{cr}}(\mathrm{kG}) r_d(\mu\mathrm{m}) = 41.37\sqrt{T_e(\mathrm{eV})/3(\mathrm{eV})}.$$

We supplement Eqs. (1)–(13) with the following boundary conditions at the sheath edge ($z=0$):

$$v_{ex,y,z} = v_{ix,y} = v_{dx,y} = 0, \quad v_{iz} = 1.5 c_{is}, \quad v_{dz} = 3 c_{ds}, \tag{24}$$

$$\phi = 0, \quad \frac{d\phi}{dz} = -\frac{m_i}{e}(\nu_{in} + \nu_{id}^e) v_{iz}.$$

Here, $c_{is}=\sqrt{T_e/m_i}$ and $c_{ds}=\sqrt{ZT_e/m_d}$ are the ion-acoustic and dust-acoustic velocities, respectively. $Z=r_d T_e/e^2$ is the charge number of the dust particle when its surface potential is equal to T_e/e.

Using the boundary conditions, we assume that the electron drift velocity at the sheath edge is smaller than the electron thermal velocity, i.e., the electrons are about Boltzmann distributed at $z=0$. It is assumed that ions and dust particles in the plasma region are accelerated mainly in the z-direction, i.e., their x- and y-velocity components are small as compared with the component in the z-direction. The expression for the potential gradient $d\phi/dz$ at $z=0$ is obtained from Eq. (9), assuming that the nonlinear term with respect of v_{iz} $(m_i v_{iz} dv_{iz}/dz)$ as well as the term $(T_i/n_i)(dn_i/dz)$ at $z=0$ are small comparing with the electric field force and/or the friction forces. The ion and dust particle velocities at the sheath edge are chosen in such way to provide an equilibrium state of the sheath structure.

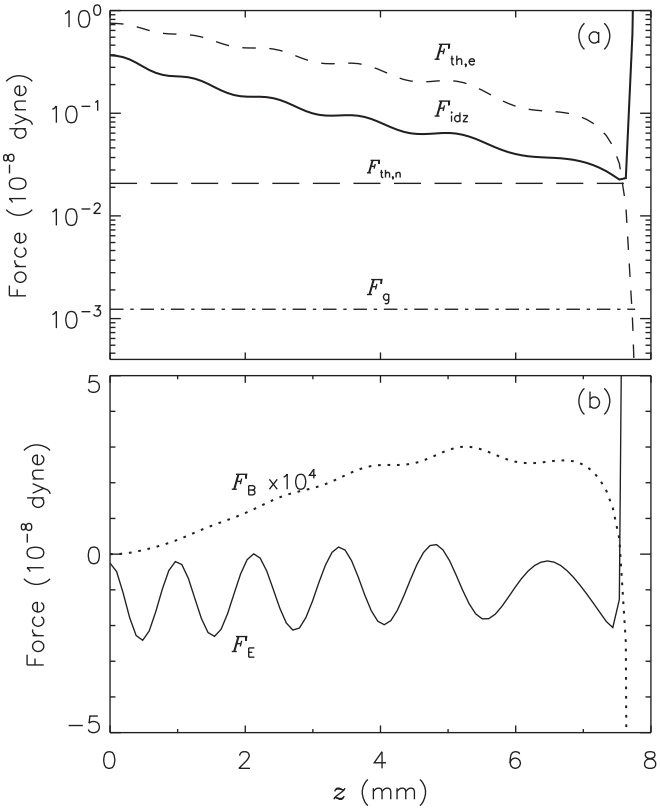

FIG. 2. The spatial distributions of the forces affecting dust particles: (a) The thermophoretic forces, $F_{\mathrm{th},e}$ and $F_{\mathrm{th},n}$, associated with electron temperature gradient (dashed curve) and neutral temperature gradient (long dashed curve), the ion drag force component F_{idz} (solid curve), and the gravitational force F_g (dashed-dotted curve). (b) The magnetic force F_B (dotted curve) and the electric force F_E (solid curve). The curves are obtained for $T_i(z=0)=0.05$ eV, $T_e(z=0)=3$ eV, $n_{e0}=10^{10}$ cm^{-3}, $p_0=1$ mTorr, $n_{d0}\approx 2.8\times 10^7$ cm^{-3}, $\nabla_z T_e=-40$ K cm^{-1}, $\nabla_z T_n=-20$ K cm^{-1}, $r_d=100$ nm, and $\rho_d=3$ g cm^{-3}.

The set of Eqs. (1)–(13) with boundary conditions (24) are solved numerically using a fourth-order Runge–Kutta method. Simultaneously, the dust charge as a function of plasma parameters is found from Eq. (20), using the step-by-step method. Starting from $z=0$, we march in space until the requirement $\phi=\phi_w$ is fulfilled. It also allows us to determine the sheath thickness.

III. NUMERICAL RESULTS

In this section, we will study the spatial distributions of the sheath parameters (the electron, ion and dust particle number densities and their velocities, the electric field potential, the forces affecting dust particles, the dust particle charge, and the sheath size). It will be found how the parameters depend on dust-plasma collisions, dust particle radius, dust particle mass density, neutral gas pressure and temperature, and electron temperature gradient. The spatial distributions will be obtained from Eqs. (1)–(13), assuming that the normalized wall potential has a fixed value (here, $e\phi_w/T_e=-10$).

Most of the results, presented in this section, are obtained for the ion temperature at the sheath edge $T_i(z=0)=0.05$ eV, which is assumed to be equal to the gas

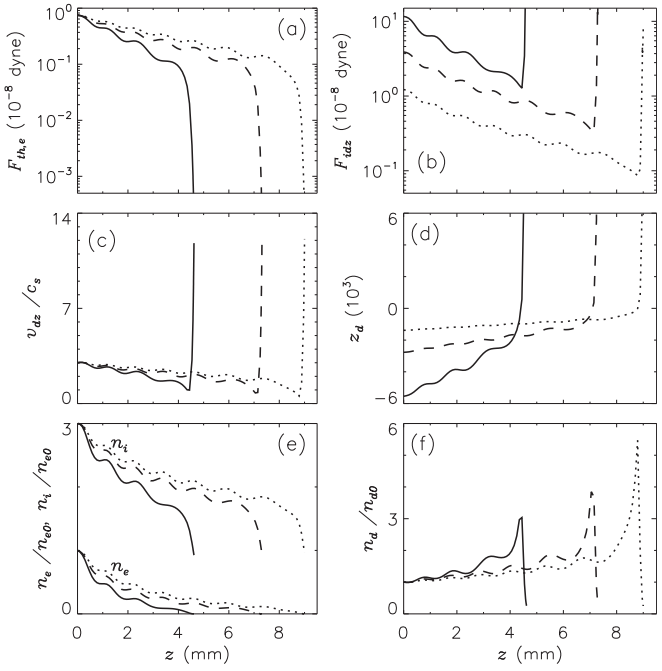

FIG. 3. The sheath parameters as functions of the z-coordinate for different dust radii: r_d=200 nm (dotted curve), 400 nm (dashed curve), and 800 nm (solid curves). The other parameters are the same as in Fig. 2.

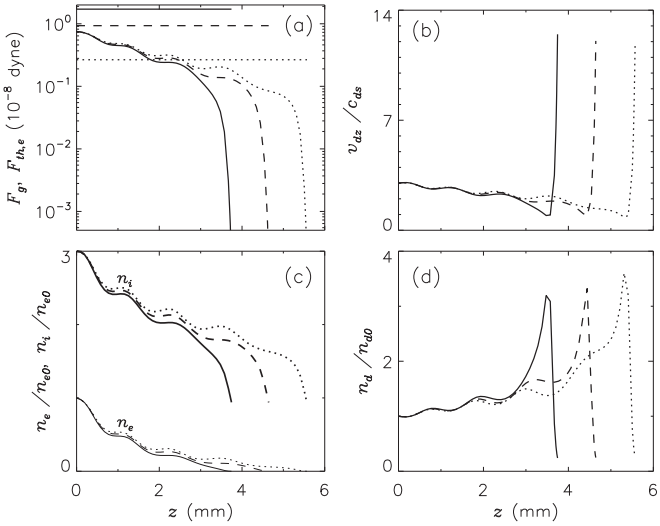

FIG. 4. The gravitational and thermophoretic forces (a), the dust particle velocity (b), the electron and ion densities (c), and the dust density (d) as functions of the z-coordinate for different dust material densities: ρ_d=3 g cm^{-3} (dotted curves), 10.50 g cm^{-3} (dashed curves), and 19.32 g cm^{-3} (solid curves), respectively. In (a), the lines which are parallel to the z-axis correspond to the gravitational force. Here, r_d=600 nm and the other parameters are the same as in Fig. 2.

temperature $T_n(z=0)$, the electron temperature at the sheath edge $T_e(z=0)=3$ eV, the electron density at the edge $n_{e0}=10^{10}$ cm^{-3}, the neutral gas pressure $p_0=1$ mTorr, the edge dust density $n_{d0}\approx 2.8\times 10^7$ cm^{-3}, the electron temperature gradient $\nabla_z T_e=-40$ K cm^{-1}, the neutral temperature gradient $\nabla_z T_n=-20$ K cm^{-1}, the dust particle radius $r_d=100$ nm, and the dust material density $\rho_d=3$ g cm^{-3}.

First, study the forces affecting dust particles in the sheath and determine what forces are most important. In Fig. 2, the spatial distributions of the forces $F_{\mathrm{th},e}$, $F_{\mathrm{th},n}$, $F_{idz}(=F_{idz}^{\mathrm{coll}}+F_{idz}^{\mathrm{orb}})$, $F_g(=m_d g)$, $F_B[=-eZ_d(B/c)v_{dy}\sin(\theta)]$, and $F_E(=-eZ_d d\phi/dz)$ are shown. One can see from the figure that the thermophoretic force $F_{\mathrm{th},e}$ and the electric force F_E are the most important forces affecting dust grains. Meanwhile, near the wall the ion drag force and the thermophoretic force associated with neutral temperature gradient may be comparable or even larger than the thermophoretic force $F_{\mathrm{th},e}$. The ion drag force is large near the wall due to enlargement of the ion drift velocity. The thermophoretic force associated with neutral temperature gradient is spatially independent for the parameters considered here. The thermophoretic forces, the ion drag force, as well as the gravitational force are accelerating dust particles toward the wall. If dust particles are negatively charged, the electric force is directed to the plasma bulk, and the Lorentz force component F_B is directed toward the wall. Near the wall, where dust particles are positively charged [see Fig. 3(d)], the Lorentz force accelerates them to the plasma bulk, and the electric force is directed toward the wall.

Since the electron and ion currents to dust grains depend on dust particle radius [see Eqs. (21) and (22)], the dust charge is a function of r_d. Therefore, investigate now how the sheath parameters depend on dust particle radius. In Figs. 3(a)–3(f), the spatial distributions of the forces $F_{\mathrm{th},e}$, F_{idz}, the dust charge, the dust particle velocity, and the electron, ion, and dust particle densities for different dust particle radii (r_d=200, 400, and 800 nm) are shown. It is found that the sheath size decreases with increasing r_d. The decrease is due to enhancement of electron collection by dust particles with increasing r_d. As a result of the enhancement, the electron density drops faster with the z-coordinate [Fig. 3(e)], and the dust charge at $z=0$ increases [see Fig. 3(e)]. Since an increase of r_d is also accompanied by enhancement of ion collection by dust particles, the ion density decreases faster when dust size becomes larger. Due to the faster decrease of n_e, the thermal force associated with electron temperature gradient also decreases faster with the z-coordinate. Meantime, the z-component of the ion drag force at $z=0$, which is proportional to r_d^2, increases, when dust size becomes larger. Due to the increase of the ion drag force component, the points, where the sum of the forces affecting dust grains is about zero, are located closer to the plasma-sheath boundary at larger r_d [see Fig. 3(c)]. In the points, the dust density is maximal, and the dust particle velocity is about zero. Therefore, the dust velocity drops faster, and the density n_d increases faster with z-coordinate, if dust radius increases. One can also see from Fig. 3 that the sheath parameters are oscillating in space. The space oscillations are due to the stratification of the dust particles, which is a result of balance between different forces affecting dust grains.[28]

The sheath parameters also depend on dust material density. In Figs. 4(a)–4(d), the gravitational force, the thermophoretic force associated with electron temperature gradient, the z-component of the dust particle velocity, and the electron, ion, and dust particle densities as functions of z-coordinate are shown for r_d=600 nm and different dust material densities ρ_d=3, 10.50, and 19.32 g cm^{-3}. These

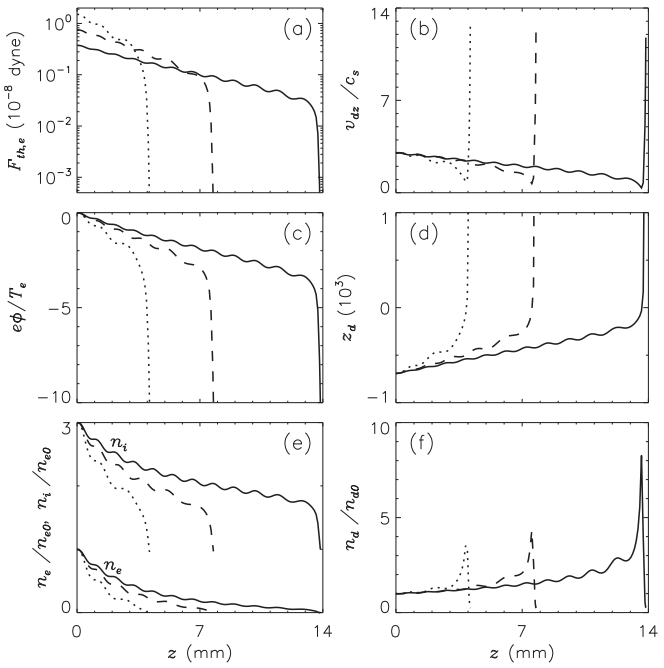

FIG. 5. The force $F_{\mathrm{th},e}$ (a), the normalized dust particle velocity (b), the normalized electric field potential (c), the dust charge (d), the normalized electron and ion densities (e), and the normalized dust particle density (f) as functions of the z-coordinate for different gas pressures: p_0=0.5 mTorr (dotted curves), p_0=1 mTorr (dashed curves), and p_0=2 mTorr (solid curves). The other parameters are the same as in Fig. 2.

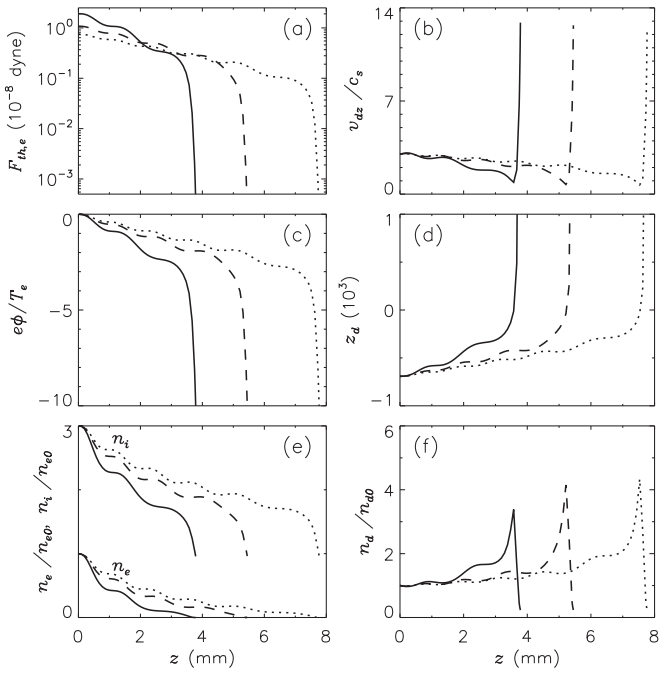

FIG. 6. The same as in Fig. 5 for different ion temperatures: T_i=0.05 eV (dotted curves), T_i=0.06 eV (dashed curves), and T_i=0.08 eV (solid curve). The other parameters are the same as in Fig. 5.

densities correspond to silicon, silver, and gold materials, respectively. The sheath size decreases with increasing ρ_d [see Figs. 4(a)–4(d)]. In our opinion, the decrease is due to enlargement of the gravitational force [Fig. 4(a)]. At larger gravitational forces, the points, where the dust particles are in equilibrium, are closer to the plasma-sheath boundary [Fig. 4(b)]. At large ρ_d, the equilibrium is mainly due to balance between the gravitational and electric forces.

Next, let us study how neutral gas pressure affects the sheath parameters. An increase of neutral gas pressure at a fixed gas temperature is accompanied by enlargement of the neutral gas density n_n. As a result of n_n increase, the thermal force associated with electron temperature gradient at z=0 drops [Fig. 5(a)]. A variation of $F_{\mathrm{th},e}$ affects the location of the points, where the sum of all the forces affecting a dust particle is about zero, and a dust particle is about in equilibrium ($v_{dz}\approx 0$). Since the force $F_{\mathrm{th},e}$ at z=0 becomes larger with decreasing p_0, the distance between the equilibrium points and the plasma-sheath boundary (z=0) decreases. As a result of the decrease, the dust velocity component v_{dz} in the region $z<4$ cm increases with p_0 growth, and, consequently, the dust density n_d decreases. Due to the n_d decrease, the electron and ion densities in the sheath are larger at higher pressures. It explains the fact that the sheath size increases with increasing p_0. Since the electron density increases with p_0 enhancement, the magnitude of the dust charge $|Z_d|$ in the region $0<z<4$ cm also becomes larger [Fig. 5(d)], and the magnitude of the electric field potential increases more slowly with the z-coordinate [Fig. 5(c)].

Let us consider the effects of the ion temperature on the sheath parameters. It follows from the hot-ion model[27] that without an external magnetic field, neglecting by ion-neutral and ion-dust collisions, the ion number density can be fairly approximated by $n_i=n_{i0}\exp(-e\phi/T_i)$. Therefore, one expects that a decrease of the ion temperature should be accompanied by an increase of the ion density in the sheath. We found that the ion density decreases faster along the dusty sheath if the ion temperature becomes larger (see Fig. 6). We attribute the ion density decrease, as well as the decrease of n_e to enhancement of the thermophoretic force $F_{\mathrm{th},e}$ at z=0 [see Fig. 6(a)]. The thermophoretic force associated with electron temperature gradient increases due to Debye radius increase and decrease of the neutral gas density at increasing T_i for a fixed p_0. Since the average ion and electron densities in the sheath decrease with increasing T_i, the average dust charge also decreases, and the magnitude of the electric field potential increases faster along the dusty sheath [Fig. 6(c)].

Next, we study how electron-dust and ion-dust momentum-transfer collisions affect dust motion and, as a result, the sheath parameters. To understand these effects, the sheath parameters were calculated neglecting by the collisions ($\nu^e_{i,ed}$=0) and were compared with those obtained in the "normal" case ($\nu^e_{i,ed}\neq 0$). In Fig. 7, the sheath parameters as functions of z-coordinate are shown for the both cases. One can see from Fig. 7 that, due to scattering of ions on dust particles, the ion drift velocity for most of z-coordinates in the $\nu^e_{i,ed}\neq 0$ case is smaller than that for $\nu^e_{i,ed}$=0. Since the ion flux $n_i v_{iz}$ depends slightly on the z-coordinate, the ion density for most of z-coordinates in the former case is larger than that obtained at $\nu^e_{i,ed}$=0. An increase of the ion density is accompanied by decreasing the plasma Debye radius. As a result, the force $F_{\mathrm{th},e}$ in the $\nu^e_{i,ed}$=0 case is larger than that obtained at $\nu^e_{i,ed}\neq 0$ for most of the z-coordinates. Due to

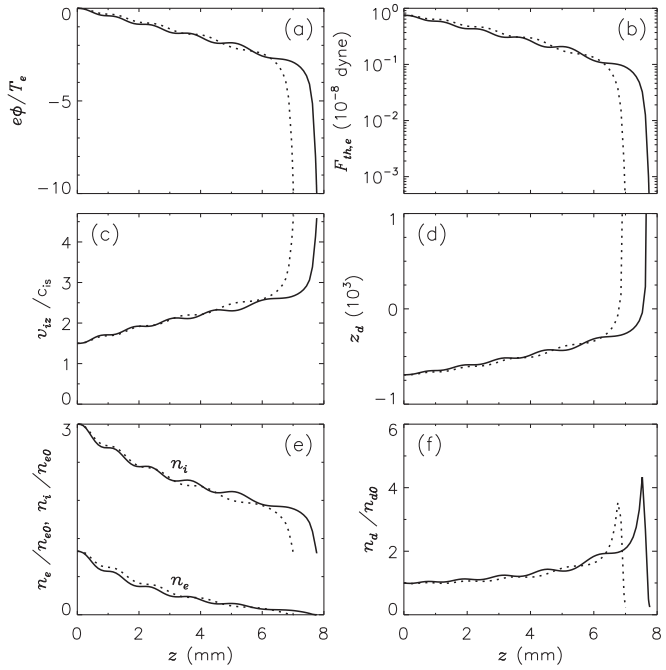

FIG. 7. The normalized electric field potential (a), the thermophoretic force $F_{\mathrm{th},e}$ (b), the z-component of the ion velocity (c), the dust charge (d), the normalized electron and ion densities (e), and the normalized dust density (f) as functions of the z-coordinate for the $\nu_{i,ed}^{e}=0$ (dotted curves) and $\nu_{i,ed}^{e}\neq 0$ (solid curves) cases. The other parameters are the same as in Fig. 2.

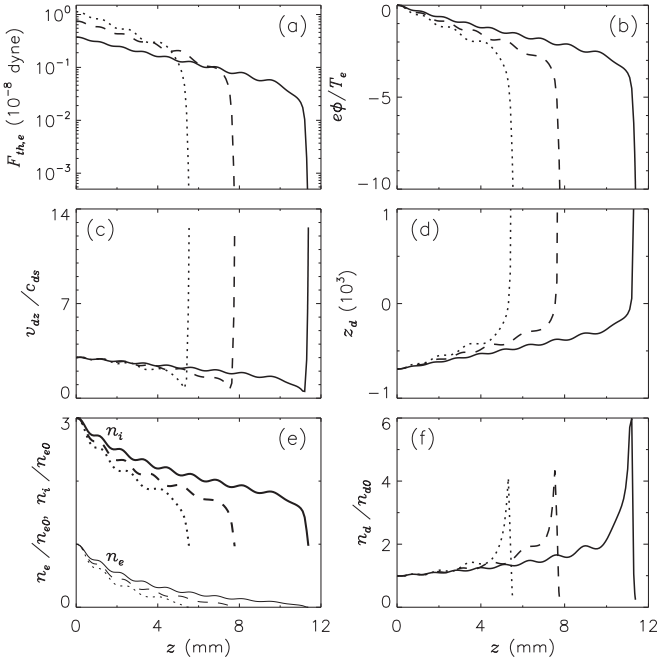

FIG. 8. The thermophoretic force $F_{\mathrm{th},e}$ (a), the normalized electric field potential (b), the z-component of the dust particle velocity (c), the dust charge (d), the normalized electron and ion densities (e), and the normalized dust density (f) as functions of the z-coordinate for different electron temperature gradients: $\nabla_z T_e=-60$ K cm^{-1} (dotted curves), $\nabla_z T_e=-40$ K cm^{-1} (dashed curves), and $\nabla_z T_e=-20$ K cm^{-1} (solid curves).

difference in the force $F_{\mathrm{th},e}$, the sheath size is larger in the normal case than that obtained for $\nu_{i,ed}^{e}=0$.

The sheath parameters also depend on the electron temperature gradient. In Fig. 8, the sheath parameters as functions of z-coordinate are shown for different electron temperature gradients: $\nabla_z T_e=-60$, -40, and -20 K cm^{-1}. It was found that the sheath size decreases with an increase of magnitude of the negative temperature gradient. This decrease may be explained by an increase of the force $F_{\mathrm{th},e}$ with increasing the gradient [Fig. 8(a)]. As a result of the force increase, the points, where $v_{dz}\approx 0$, are located closer to the plasma-sheath boundary at larger $|\nabla_z T_e|$, and the dust particle velocities at $z<5$ cm are smaller and the dust densities are larger. The enhancement of the dust density in the region $z<5$ cm is accompanied by a decrease of the electron and ion densities and, consequently, by a decrease of the negative dust charge and an increase of the magnitude of the electric field potential [see Figs. 8(b), 8(d), and 8(e)].

IV. DISCUSSION AND SUMMARY

In this section, we will discuss the results obtained in previous section and simplifications used in the model, as well as summarize the results. We have studied properties of a plasma-sheath (the sheath size, the electron, ion and dust particle densities and velocities, the electric field potential, and the forces affecting dust particles) in the presence of an oblique magnetic field for the conditions, when the thermophoretic force associated with electron temperature gradient is important among the forces affecting dust grains. The results of our studies have shown that the thermophoretic force may be important at low pressures ($\sim$1 mTorr) and relatively large electron densities ($\sim 10^{10}$ cm^{-3}), when the ratio n_e/n_n is relatively large ($\sim 10^{-3}$). Such parameters are typical for high-density plasmas operated at low pressures.[52,53] For the conditions, the thermophoretic force can be dominant among all the forces pushing negatively charged dust particles to the wall (Fig. 2). Therefore, a variation in the force may strongly affect the sheath properties. For example, a decrease of neutral gas pressure is accompanied by an increase of the force $F_{\mathrm{th},e}$ at $z=0$ and, as a result, by a decrease of the sheath width (Fig. 5). The sheath decrease is due to the fact that at larger $F_{\mathrm{th},e}(z=0)$ the location of the points, where the sum of all the forces affecting a dust grain is about zero ($v_{dz}\approx 0$), is closer to the plasma-sheath boundary [see Fig. 5(b)]. The sheath size also decreases with increasing ion and neutral temperatures because the increase is accompanied by a decrease of the neutral gas density and, consequently, by an increase at $z=0$ of the thermophoretic force associated with electron temperature gradient (Fig. 6). Since the force $F_{\mathrm{th},e}$ naturally increases with increasing the electron temperature gradient, the sheath size decreases with enhancement of the gradient, if T_e drops in direction from the bulk plasma to the wall.

Note that the thermophoretic force associated with electron temperature may be large in low-pressure plasmas only at relatively large magnetic fields because the electron thermal conductivity increases with decreasing magnetic field, and the electron temperature is nearly uniform at $B=0$.[54]

The magnetized sheath size also depends on dust particle properties. For example, an increase of dust radius is accompanied by a decrease of the sheath size due to increase of the ion drag force. At larger dust material densities, the gravita-

tional force is larger and the sheath size is smaller. Sheath size also depends on electron and ion-dust collisions. The model, which accounts for the plasma-dust collisions, gives larger sheath sizes than the model, where the collisions are neglected (Fig. 7).

Note that we have used some simplifications in the model. In particular, the expression for the thermophoretic force associated with electron temperature gradient is obtained, using qualitative estimations.[44] Additional efforts, both in theoretical and numerical modeling, to get more exact expression for the force are required. Next, the sheath model has been developed without connection with a plasma bulk model. To have a better insight in the sheath processes, one has to accompany the sheath model with an appropriate plasma bulk model. Moreover, studying the dust charging in the sheath, we neglected by the dust charge distribution[55] and dust size distribution and assumed that the electron distribution function is Maxwellian. Meanwhile, the electron energy distribution in the plasma bulk and sheath may be far away from the Maxwellian distribution.[13] However, even with these simplifications, the model provides very important information about the magnetized sheath of a dusty plasma and the methods how to control the sheath properties.

In summary, a free-component fluid model for a dusty plasma-sheath in an oblique magnetic field is presented. Using the model, effects of neutral gas pressure and ion (neutral gas) temperature, dust size and dust material density, electron temperature gradient, and plasma-dust collisions on the sheath structure are studied. The study is carried out for a low-pressure high-density plasma case, when the thermophoretic force associated with electron temperature gradient is one of the most important forces affecting dust grains in the sheath. Results of our studies show that for the parameters considered here an increase of the forces pushing dust particles to the wall is accompanied by the sheath decrease. The results of the studies may be useful for plasma technologies, where control of nano- and microsized structures in plasma-sheaths near a substrate is required.

ACKNOWLEDGMENTS

I.D. was supported by the Humboldt Foundation. This work was partially supported by CSIRO's OCE Science Leadership Program and the Australian Research Council (Australia).

[1] *Dusty Plasmas in Physics, Chemistry, and Technological Impacts in Plasma Processing*, edited by A. Bouchoule (Wiley, New York, 1999).
[2] S. V. Vladimirov and K. Ostrikov, Phys. Rep. **393**, 175 (2004).
[3] P. K. Shukla and B. Eliasson, Rev. Mod. Phys. **81**, 25 (2009).
[4] V. E. Fortov, A. V. Ivlev, S. A. Khrapak, A. G. Khrapak, and G. E. Morfill, Phys. Rep. **421**, 1 (2005).
[5] S. V. Vladimirov, K. Ostrikov, and A. A. Samarian, *Physics and Applications of Complex Plasmas* (Imperial College, London, 2005).
[6] K. Ostrikov, Rev. Mod. Phys. **77**, 489 (2005).
[7] M. S. Barnes, J. H. Keller, J. C. Forster, J. A. O'Neill, and D. K. Coultas, Phys. Rev. Lett. **68**, 313 (1992).
[8] I. B. Denysenko, M. Y. Yu, L. Stenflo, and N. A. Azarenkov, Phys. Plasmas **12**, 042102 (2005).
[9] I. Denysenko, M. Y. Yu, L. Stenflo, and S. Xu, Phys. Rev. E **72**, 016405 (2005).
[10] S. I. Popel and M. Y. Yu, Phys. Plasmas **3**, 4313 (1996).
[11] S. I. Popel and A. A. Gisko, Nonlinear Processes Geophys. **13**, 223 (2006).
[12] Ph. Belenguer, J. Ph. Blondeau, L. Boufendi, M. Toogood, A. Plain, A. Bouchoule, C. Laure, and J. P. Boeuf, Phys. Rev. A **46**, 7923 (1992).
[13] I. Denysenko, M. Y. Yu, K. Ostrikov, N. A. Azarenkov, and L. Stenflo, Phys. Plasmas **11**, 4959 (2004).
[14] I. Denysenko, M. Y. Yu, K. Ostrikov, and A. Smolyakov, Phys. Rev. E **70**, 046403 (2004).
[15] I. Denysenko, M. Y. Yu, and S. Xu, J. Phys. D **38**, 403 (2005).
[16] I. Denysenko, J. Berndt, E. Kovacevic, I. Stefanovic, V. Selenin, and J. Winter, Phys. Plasmas **13**, 073507 (2006).
[17] K. Ostrikov and A. B. Murphy, J. Phys. D **40**, 2223 (2007).
[18] Y. C. Hong, J. H. Kim, C. U. Bang, and H. S. Uhm, Phys. Plasmas **12**, 114501 (2005).
[19] L. Wang, L. Cui, X. D. Zhu, and X. H. Wen, Phys. Plasmas **14**, 123501 (2007).
[20] J. D. Long, S. Xu, J. W. Cai, N. Jiang, J. H. Lu, K. N. Ostrikov, and C. H. Diong, Mater. Sci. Eng., C **20**, 175 (2002).
[21] M. S. Bell, K. B. K. Teo, and W. I. Milne, J. Phys. D **40**, 2285 (2007).
[22] P. P. Rutkevych, K. Ostrikov, and S. Xu, Phys. Plasmas **12**, 103507 (2005).
[23] P. P. Rutkevych, K. Ostrikov, S. Xu, and S. V. Vladimirov, J. Appl. Phys. **96**, 4421 (2004).
[24] S. J. Choi and M. J. Kushner, Appl. Phys. Lett. **62**, 2197 (1993).
[25] M. Y. Yu, H. Saleem, and H. Luo, Phys. Fluids B **4**, 3427 (1992).
[26] T. Nitter, Plasma Sources Sci. Technol. **5**, 93 (1996).
[27] J. X. Ma and M. Y. Yu, Phys. Plasmas **2**, 1343 (1995).
[28] J. X. Ma, J.-Y. Liu, and M. Y. Yu, Phys. Rev. E **55**, 4627 (1997).
[29] G. C. Das and P. Kalita, J. Phys. D **37**, 702 (2004).
[30] J.-Y. Liu, Z.-X. Wang, X. Wang, Q. Zhang, X. Zou, and Y. Zhang, Phys. Plasmas **10**, 3507 (2003).
[31] M. Davoudabadi, B. Rovagnati, and F. Mashayek, IEEE Trans. Plasma Sci. **34**, 142 (2006).
[32] Yu. I. Chutov, A. Kravchenko, and P. Schram, Physica B **228**, 11 (1996).
[33] Yu. I. Chutov, O. Yu. Kravchenko, A. F. Pshenychnyj, R. D. Smirnov, K. Asano, N. Ohno, S. Takamura, and Y. Tomita, Phys. Plasmas **10**, 546 (2003).
[34] Y. N. Nejoh, Phys. Plasmas **8**, 3545 (2001).
[35] Z.-X. Wang, J.-Y. Liu, Y. Liu, and X. Wang, Phys. Plasmas **12**, 012104 (2005).
[36] M. Mikikian, C. Arnas, K. Quotb, and F. Doveil, in *Frontiers in Dusty Plasma*, edited by Y. Nakamura, T. Yokota, and P. K. Shukla (Elsevier, Amsterdam, 2000), p. 207.
[37] N. Ch. Adhikary, H. Bailung, A. R. Pal, J. Chutia, and Y. Nakamura, Phys. Plasmas **14**, 103705 (2007).
[38] B. P. Pandey, A. Samarian, and S. V. Vladimirov, Phys. Plasmas **14**, 093703 (2007).
[39] M. Davoudabadi and F. Mashayek, Phys. Plasmas **12**, 073505 (2005).
[40] I. Beilis and M. Keidar, Phys. Plasmas **5**, 1545 (1998).
[41] S. K. Baishya, G. C. Das, J. Chutia, and J. Sarma, Phys. Plasmas **6**, 3678 (1999).
[42] G. Foroutan, H. Mehdipour, and H. Zahed, Phys. Plasmas **16**, 103703 (2009).
[43] H. Mehdipour and G. Foroutan, Phys. Plasmas **17**, 083704 (2010).
[44] J. E. Daugherty and D. B. Graves, J. Appl. Phys. **78**, 2279 (1995).
[45] K. N. Ostrikov, M. Y. Yu, and N. A. Azarenkov, J. Appl. Phys. **84**, 4176 (1998).
[46] N. A. Azarenkov, I. B. Denisenko, and K. N. Ostrikov, J. Phys. D **28**, 2465 (1995).
[47] K. N. Ostrikov, M. Y. Yu, and H. Sugai, J. Appl. Phys. **86**, 2425 (1999).
[48] M. A. Lieberman and A. J. Lichtenberg, *Principle of Plasma Discharges and Material Processing* (Wiley, New York, 1994).
[49] C. Yamabe, S. J. Buckman, and A. V. Phelps, Phys. Rev. A **27**, 1345 (1983).
[50] S. A. Khrapak, S. V. Ratynskaia, A. V. Zobnin, A. D. Usachev, V. V. Yaroshenko, M. H. Thoma, M. Kretschmer, H. Höfner, G. E. Morfill, O. F. Petrov, and V. E. Fortov, Phys. Rev. E **72**, 016406 (2005).
[51] V. N. Tsytovich, N. Sato, and G. E. Morfill, New J. Phys. **5**, 43 (2003).

[52]K. N. Ostrikov, S. Xu, and A. B. M. S. Azam, J. Vac. Sci. Technol. **20**, 251 (2002).
[53]S. Xu, K. N. Ostrikov, W. Luo, and S. Lee, J. Vac. Sci. Technol. **18**, 2185 (2000).
[54]N. A. Azarenkov, I. B. Denysenko, A. V. Gapon, and T. W. Johnston, Phys. Plasmas **8**, 1467 (2001).
[55]I. B. Denysenko, K. Ostrikov, S. Xu, M. Y. Yu, and C. H. Diong, J. Appl. Phys. **94**, 6097 (2003).